ELSEVIER

Biochimica et Biophysica Acta 1561 (2002) 147–158

BIOCHIMICA ET BIOPHYSICA ACTA
BBA

www.bba-direct.com

Biophysical consequences of linker chemistry and polymer size on stealth erythrocytes: size does matter

Amanda J. Bradley [a,b], Kari L. Murad [a,c], Katy L. Regan [a], Mark D. Scott [a,b,*]

[a] *Center for Immunology and Microbial Disease, Albany Medical College, Albany, NY, USA*
[b] *Canadian Blood Services, Department of Pathology and Laboratory Medicine, Koerner Pavilion, U.B.C. Hospital, University of British Columbia, 2211 Wesbrook Mall, Vancouver, BC, Canada V6T 2B5*
[c] *Department of Physical and Biological Sciences, College of St. Rose, Albany, NY, USA*

Received 29 August 2001; received in revised form 11 December 2001; accepted 18 December 2001

Abstract

Immunocamouflaged red blood cells (RBC) are produced by cell surface derivatization with methoxypolyethylene glycol (mPEG). These immunologically attenuated cells may reduce the risk of allosensitization in chronically transfused patients. To characterize the effects of differing linker chemistries and polymer lengths, RBC were modified with cyanuric chloride activated mPEG (C-mPEG 5 kDa), benzotriazole carbonate methoxyPEG (BTC-mPEG; 5 or 20 kDa) or *N*-hydroxysuccinimidyl ester of mPEG propionic acid (SPA-mPEG; 2, 5 or 20 kDa). Biophysical methods including particle electrophoresis and aqueous two-phase polymer partitioning were employed to compare the PEG derivatives. While C-mPEG was faster reacting, both BTC-mPEG and SPA-mPEG gave comparable findings after 1 h. Both PEG surface density and molecular mass had a large effect on RBC surface properties. Proportional changes in electrophoretic mobility and preferential phase partitioning were achieved by increasing either the quantity of surface PEG or the PEG molecular mass. In addition, two-phase partitioning may provide a means for efficiently removing unmodified or lightly modified (hence potentially immunogenic) RBC in the clinical setting. Furthermore, mPEG modification significantly inhibits cell–cell interaction as evidenced by loss of Rouleaux formation and, consequently, sedimentation rate. Importantly, BTC-mPEG 20 kDa RBC showed normal in vivo survival in mice at immunoprotective concentrations (up to 2 mM).

Keywords: Polyethylene glycol; Erythrocyte; Linker; Immunomodulation; Transfusion; Alloimmunization

1. Introduction

Methoxypolyethylene glycol (mPEG) is a neutral, non-toxic polymer that has been covalently grafted to proteins, biomaterials and cell surfaces as a means of improving biocompatibility and reducing immunological recognition. Examples of PEG-modified agents include therapeutic proteins such as interleukin 2 for anti-tumor effects [1], streptokinase for anti-thrombosis [2], liposomes for enhanced drug and gene delivery [3] and, most recently, mPEG-derivatized erythrocytes and lymphocytes [4–6].

mPEG-erythrocytes have been previously characterized and were found to be morphologically and functionally normal and, at immunoprotective levels, to have normal in vivo survival in mouse models.

* Corresponding author, at address b. Fax: 604-822-7635.
E-mail address: mscottpath@aol.com (M.D. Scott).

0005-2736/02/$ – see front matter
PII: S0005-2736(02)00339-5

More importantly, mPEG modification significantly reduced the antigenicity of human red blood cells (RBC) with respect to non-ABO blood group antigens and dramatically diminished the immunogenicity of allogeneic and even xenogeneic RBC in mouse models [4,5]. As a consequence of this immunocamouflage, mPEG-modified RBC may significantly attenuate the risk of alloimmunization for patients requiring chronic RBC transfusions such as patients with sickle cell anemia and thalassemias. This is particularly important since as many as 35% of individuals with sickle cell disease or thalassemias exhibit clinically significant alloimmunization to non-ABO antigens [7,8]. In this clinical setting, the immunocamouflaged mPEG-RBC would be most beneficial in providing a safe, functional transfusion product.

To date, the majority of studies on PEGylated RBC have employed cyanuric chloride activated mPEG (C-mPEG) with a molecular mass of 5 kDa. However, because both the density of attached PEG as well as the mPEG chain length have been hypothesized to alter the efficacy of the immunocamouflage [4,9], we have assessed alternative mPEG derivatives of varying molecular mass. Like C-mPEG, both mPEG-benzotriazolyl carbonate (BTC-mPEG; 5 and 20 kDa) and mPEG succinimidyl propionate (SPA-mPEG; 2, 5 and 20 kDa) react predominantly with the ε-amino groups of lysine residues and to a lesser extent with amino-terminal groups in proteins. However, unlike C-mPEG which introduces a triazine ring between mPEG and the protein, BTC- and SPA-mPEG attach mPEG to the target in the form of a stable amide bond. Utilizing these different derivatives of mPEG, the efficiency of the PEG-RBC linkage reaction and the efficacy of immunocamouflage were assessed.

2. Materials and methods

2.1. Blood collection

Following informed consent, whole blood was drawn from normal healthy volunteers into heparin Vacutainer tubes. Erythrocytes were obtained by washing three times with saline. Murine RBC were collected in heparinized syringes from Balb/c mice via cardiac bleed.

2.2. PEG derivatives

BTC-mPEG (5 and 20 kDa) and *N*-hydroxysuccinimidyl ester of mPEG propionic acid (SPA-mPEG; 2 and 20 kDa) were obtained from Shearwater Polymers (Huntsville, AL, USA). SPA-mPEG 5 kDa was purchased from Fluka Chemie (Sigma-Aldrich, St. Louis, MO, USA). Cyanuric chloride activated mPEG (C-mPEG; 5 kDa) was purchased from Sigma. Bifunctional PEG derivatives, polyethylene glycol-bis-benzotriazolyl carbonate (BTC-PEG-BTC) and the succinimidyl ester of polyethylene glycol-bis-propionic acid (SPA-PEG-SPA) (PEG of 3.4 kDa), were obtained from Shearwater Polymers. Derivatives were used without further purification or purity assessment. Derivatives from Shearwater were $>95\%$ pure. C-mPEG had $<1\%$ free cyanuric chloride present.

2.3. PEG derivatization

Erythrocytes were modified either as whole blood or as washed cells at a 12% or a 20% hematocrit as previously described [4,10]. Briefly, stock solutions of PEG derivatives were made in 50 mM dibasic potassium phosphate, 105 mM NaCl, pH 8.0 (PEG buffer). Overall mPEG concentrations ranged from 0 mM to 7.5 mmol/l. Derivatization reactions were carried out at room temperature for either 30 min or 1 h according to the reactivity of the derivative. Modified RBC were then washed three times with saline. Control groups consisted of both untreated saline washed RBC and RBC incubated in mPEG-free PEG buffer (0 mM mPEG-RBC).

2.4. Anti-A antibody-mediated RBC agglutination

This assay was used to assess the ability of attached mPEG to inhibit anti-A antibody-mediated agglutination. Briefly, 450 μl of control or pegylated RBC (blood type A) suspensions (6% hematocrit in isotonic saline) were placed in an aggregometer cuvette at 37°C, with stirring, and 20 μl of anti-A typing serum (or pooled human antiserum) was added. RBC aggregation was then followed over time using a platelet aggregometer as previously described [4].

2.5. Cell–cell interaction

In vitro and in vivo, RBC self-associate giving rise to RBC 'stacks' (Rouleaux formation). In turn, this Rouleaux formation underlies the sedimentation rate used clinically. To assess this natural cell–cell interaction, sedimentation rate and Rouleaux formation were measured for control and PEGylated RBC. For analysis of sedimentation rate, control and mPEG-RBC were suspended to a 40% hematocrit in autologous plasma and loaded into erythrocyte sedimentation tubes (Winpette, Fisher Scientific, Pittsburgh, PA, USA). RBC sedimentation rate was then monitored over a 5 h period. Simultaneously, aliquots of the control and mPEG-derivatized RBC were mixed with equal amounts of either autologous plasma or a 1% saline-buffered dextran solution (dextran molecular mass $\sim$500 kDa, from Pharmacia, Uppsala, Sweden) (to induce Rouleaux formation) and examined microscopically for Rouleaux formation.

2.6. In vivo survival of mPEG-modified RBC

To evaluate the effects of the various mPEG derivatives in vivo, RBC survival studies were performed in Balb/c mice. RBC were collected from donor mice via cardiac bleed and derivatized with BTC-mPEG (20 kDa) as previously described [4,5]. The concentration of mPEG used for the in vivo studies ranged from 0 to 2 mmol/l since murine RBC are physically smaller (i.e. have fewer surface binding sites for mPEG) and more fragile than human RBC. Murine RBC were labeled using the fluorescent, membrane anchored marker PKH-26 (Sigma). Blood samples from recipient mice were followed until the labeled RBC were cleared from circulation (approx. 40–50 days for unmodified syngeneic cells). Survival of fluorescently labeled mPEG-treated and control RBC was monitored by analyzing the percentage of fluorescently labeled RBC by flow cytometry. A minimum of five mice were used for each mPEG concentration tested.

2.7. Biophysical determinations

To directly measure the effects of linker chemistry and polymer size, biophysical comparisons of the control and mPEG-derivatized RBC were done via partitioning in an aqueous two-phase polymer system and particle electrophoresis. These techniques have been used previously to monitor the consequences of PEG derivatization of proteins and the incorporation of PEG into liposomes [11–13]. Similarly, these techniques have also been extensively used to study erythrocyte surface properties [14,15]. Partitioning in an aqueous two-phase polymer system (which forms due to the immiscibility of the two polymers: PEG and dextran) exploits the affinity of PEG-RBC for the PEG-rich upper phase. Unmodified as well as poorly derivatized RBC remain at the interface or within the dextran layer. Particle electrophoresis measures the mobility of particles (e.g. RBC) in an applied electric field. PEG-mediated changes to the RBC surface are detected as a reduction in electrophoretic mobility due to the camouflage of RBC surface charge and the increased drag force of the polymer itself.

2.8. Partitioning

Partitioning of control and PEG-modified RBC was carried out in an aqueous two-phase system consisting of PEG8000 (Sigma) and dextran T500 (molecular mass $\sim$500 kDa; Pharmacia). The two-phase system denoted (5,4) was prepared as described previously [16,17] and consisted of 5% (w/w) dextran, 4% (w/w) PEG, 0.15 M NaCl, 6.84 mM Na_2HPO_4, and 3.16 mM NaH_2PO_4 (pH 7.4). PEG and dextran stock solution concentrations were determined by refractive index measurements. Phase systems were made up in 50 ml polypropylene tubes and allowed to equilibrate overnight at room temperature. The upper (PEG-rich) phase was drawn off into a separate tube and the lower (dextran-rich) phase was obtained by puncturing the tube to collect the solution. Phase systems were used within 3 days. Control and PEG-RBC were labeled with ^{51}Cr to allow for quantitation. The partitioning experiment was performed in duplicate and consisted of the addition of 12 μl (load) of ^{51}Cr-RBC (3.7×10^8/ml) to 0.75 ml each of the upper and lower phases. Tubes were inverted 20 times and the phases were allowed to equilibrate and separate at room temperature for 20 min. Aliquots (350 μl) from both phases were removed for γ-counting. Results were expressed as the percentage of ^{51}Cr-

RBC in the upper phase relative to the total ^{51}Cr-labeled cells added to the system.

2.9. Particle electrophoresis

Mobility measurements for control and PEG-RBC were made using the Rank Mark I electrophoresis apparatus equipped with a horizontal microscope with a water immersion lens [13,18]. Ten different RBC were chosen randomly and were timed to determine their velocity in the electric field. The electrophoretic mobility was determined as: mobility = velocity of the particle (μm/s)/electric field strength (E) in V/cm, where E = (voltage/distance between the electrodes).

3. Results

As previously reported, at immunoprotective levels of derivatization, all of the monofunctional mPEG moieties yielded morphologically normal RBC as assessed by both microscopic and Coulter counter analysis (data not shown; [4,5,19]). This finding was observed following mPEG derivatization of both washed RBC and whole blood RBC. Only at relatively high concentrations (>2 mmol/l) of derivatization with BTC-mPEG 20 kDa did the cells appear slightly crenated. In contrast, the bifunctional derivatives proved to be less useful for our purposes since significant, spontaneous, aggregation of the RBC resulted due to cross-linking of individual RBC.

Initial studies examined the differential effects of modifying whole blood versus washed RBC. Not surprisingly, since whole blood contains large amounts of competing derivatization substrates (lymphocytes, plasma proteins, and platelets), derivatization was more efficient using washed RBC versus whole blood at equimolar C-mPEG concentrations. As shown in Fig. 1A, type A RBC agglutination was inhibited to a greater extent following derivatization of washed RBC as compared with derivatized whole blood.

The direct relationship between the RBC:mPEG derivative ratio, the efficacy of linker chemistry, the extent of cell modification, and the effect of polymer size was evident following two-phase partitioning. Following extensive studies, a (5,4) (dextran, PEG) system was found to be ideal for assessing and com-

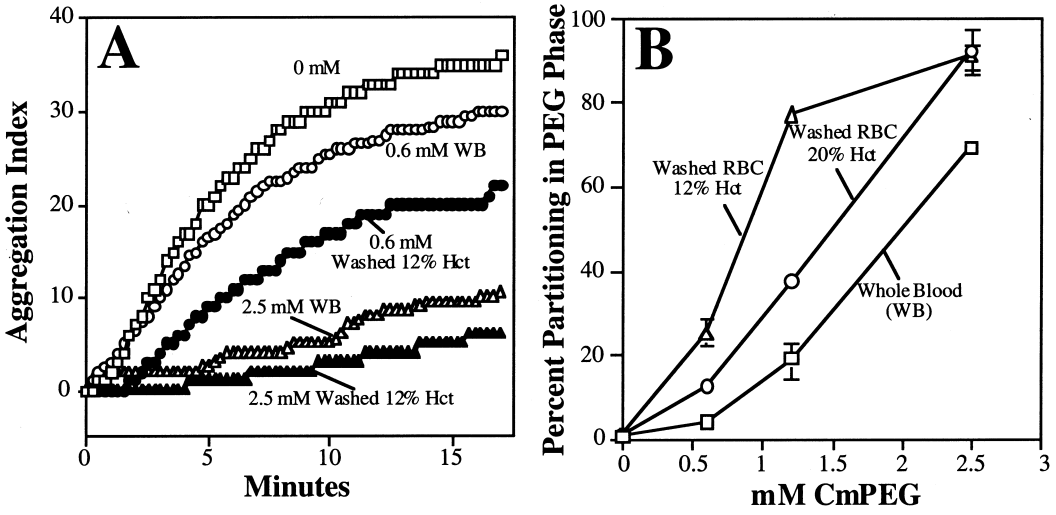

Fig. 1. Greater mPEG attachment levels are achieved by modifying washed erythrocytes compared to whole blood. Erythrocytes were modified with C-mPEG 5 kDa in whole blood (WB) or as washed cells (at either 20% or 12% hematocrit) for 30 min at room temperature, pH 8.0. Concentrations of C-mPEG refer to the amount of C-mPEG reacted with RBC (not the amount attached). (A) Aggregation of A-RBC in the presence of anti-A antisera illustrated the extent of mPEG modification obtained. As mPEG modification increased, the amount of aggregation decreased since attached mPEG inhibits cell–cell interactions. Shown is a representative experiment from three independent assays. (B) Different mPEG modification levels were also evident by partitioning in aqueous two-phase systems. As the amount of attached mPEG increased, the percent of RBC partitioning in the upper, PEG-rich phase also increased. Symbols show the mean data for three experiments, each done in duplicate ±1 S.D.

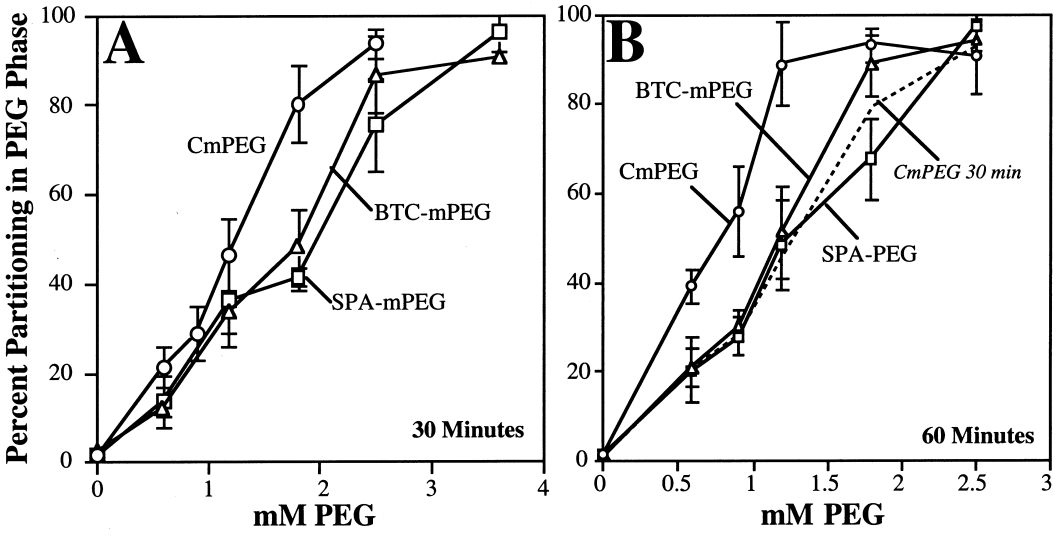

Fig. 2. The C-mPEG derivative reacts faster than BTC- or SPA-mPEG in grafting mPEG to the RBC membrane. RBC (washed and at a 12% hematocrit) were modified with mPEG 5 kDa derivatives: C-mPEG, BTC- or SPA-mPEG for either 30 min (A) or for 1 h (B) at room temperature, pH 8. Control and modified RBC were partitioned in the (5,4) aqueous two-phase system. Symbols show the mean data for three experiments, each done in duplicate. Error bars are 1 S.D. Data for RBC modified with C-mPEG for 30 min are included in panel B for ease of comparison.

paring changes in RBC membrane derivatization. In this two-phase system, only about 1% of unmodified RBC partition to the upper PEG-rich phase while ~65% remain at the PEG–dextran interface and 34% are in the dextran-rich phase. As expected, the transition of RBC from the interface/dextran layer to the PEG-rich upper phase was a function of mPEG derivative concentration, protein concentration (washed RBC versus whole blood), and cell number (hematocrit) (Fig. 1B). While 77% of modified washed RBC (12% hematocrit) partitioned into the upper PEG phase following derivatization with 1.2 mmol/l, only 19% of RBC from whole blood were observed in the PEG-rich layer. Indicative of the relationship between mPEG derivative concentration per RBC, modification of higher hematocrits of washed RBC yielded progressively lowered partitioning into the PEG-rich layer. For example, derivatization of a 20% hematocrit with 1.2 mmol/l C-mPEG resulted in 38% of the RBC partitioning to the upper PEG phase.

The two-phase partitioning system was also employed to assess whether any differences in reaction rates and overall membrane derivatization existed between the three chemical linker agents. As noted in Fig. 2A, C-mPEG more rapidly derivatized RBC when compared to either the BTC- or SPA-mPEGs. To obtain an upper PEG phase partition of 50% after 30 min of reaction time, less C-mPEG 5 kDa (1.2 mM) was required compared with BTC- or SPA-mPEG 5 kDa (1.8 mM). After a 1 h reaction time, less than 0.9 mM C-mPEG was required compared to 1.2 mM BTC- or SPA-mPEG 5 kDa to give an upper PEG phase partition of 50% (Fig. 2B). The greater reactivity of C-mPEG was also demonstrated via microaggregometry in that less C-mPEG (e.g. 0.6 mmol/l C-mPEG 5 kDa versus 1.2 mmol/l BTC- or SPA-mPEG 5 kDa) was required to achieve significant (>50%) inhibition of antiserum-mediated agglutination (data not shown). However, while BTC and SPA-mPEGs react more slowly with RBC than C-mPEG, equivalent partitioning was noted after 1 h of derivatization (Fig. 2B).

In addition to PEG surface density, the molecular mass of the mPEG derivative also had an enormous effect on RBC surface properties as determined by both partitioning and particle electrophoresis (Figs. 3 and 4). Aqueous two-phase partitioning data confirmed the very strong mPEG derivative molecular mass effect (Fig. 3). To achieve ~50% partitioning into the upper phase, only 0.3–0.45 mM mPEG 20 kDa (BTC or SPA) was required compared to 1.2 mM mPEG 5 kDa derivatives or 2.5 mM SPA-mPEG 2 kDa. To achieve over 80% partitioning

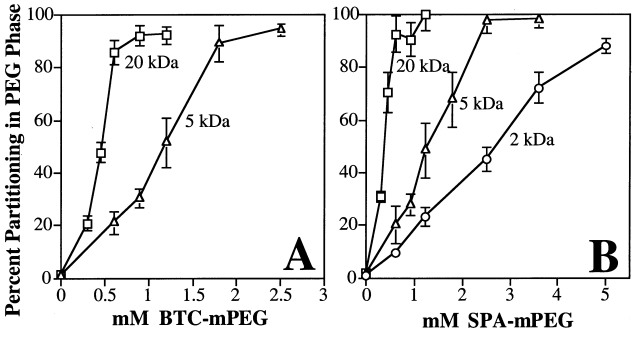

Fig. 3. Effect of linker chemistry and polymer size on aqueous two-phase partitioning of mPEG-modified RBC. Shown is a comparison of the phase partitioning of BTC-mPEG (5 and 20 kDa) and SPA-mPEG (2, 5 and 20 kDa). (A) RBC partitioning into the PEG-rich phase increases in an mPEG dose-dependent manner. Partitioning is further enhanced by increasing polymer length (molecular mass). (B) Similar partitioning results were obtained with the SPA derivatives. Again, note the dramatic and significant effect that polymer length has at equimolar concentrations of derivatization. RBC were derivatized as washed cells at a 12% hematocrit for 1 h at room temperature. Symbols show the mean data ±1 S.D. for duplicate samples from three independent experiments.

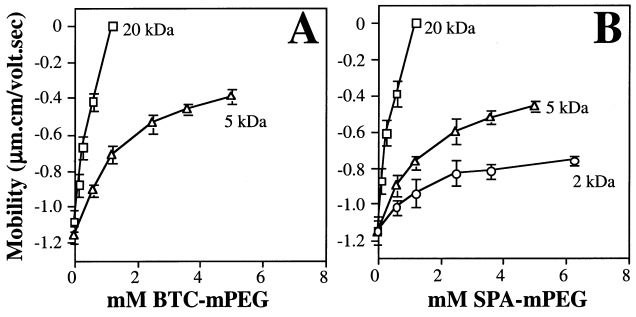

Fig. 4. Electrophoretic mobility is decreased consequent to immunocamouflage. Shown is a comparison of the electrophoretic mobility of control and BTC-mPEG (A; 5 and 20 kDa) and SPA-mPEG (B; 2, 5 and 20 kDa) derivatized human RBC. RBC electrophoretic mobility is a function of the membrane surface charge and the drag coefficient of the RBC itself. Under the conditions used, normal human RBC have a mobility of approx. −1.18 μm·cm/V·s. As shown, mPEG derivatization results in the immunocamouflage of the inherent surface charge of the RBC resulting in the loss of electrophoretic mobility. The efficacy of the immunocamouflage is a function of polymer density (mM) and polymer length (kDa). As the mPEG molecular mass and derivatization concentrations increased, a greater shift in mobility towards zero was observed. Complete neutralization of the electrophoretic mobility is noted at very low derivatization concentrations of the 20 kDa BTC- and SPA-mPEGs. RBC were modified as washed cells at a 12% hematocrit for 1 h at room temperature. The electrophoretic mobilities of control and mPEG-modified cells were determined using measurements for 10 RBC per experiment. Symbols show the mean of two independent experiments ±1 S.D.

into the PEG phase, 0.6 mM SPA/BTC-mPEG 20 kDa or ∼2 mM SPA/BTC-mPEG 5 kDa or 5 mM SPA-mPEG 2 kDa were required. Assessing the effect of molecular mass in terms of the total number of ethoxy units, slightly more of the 20 kDa PEG derivatives were required to achieve equivalent affinity partitioning. The ratio of ethoxy units required for 50% affinity partitioning was ∼(1:1.2:1.2–1.8) for the PEG 2 kDa ($n=45$):PEG 5 kDa ($n=113$):PEG 20 kDa ($n=454$) respectively, where n is the number of ethoxy units per molecule. To achieve 80% affinity partitioning, the ratio was (1:1:1.2).

These partitioning findings are of importance since a key clinical requirement for the use of PEGylated RBC in the prevention of alloimmunization will be

Table 1
Separation of mPEG-modified erythrocytes from unmodified cells is efficiently accomplished via two-phase partitioning

Cell types	Mixture: percent mPEG-derivatized cells (mean ± S.D.)				
	10	30	50	70	90
C-mPEG 5 kDa	9.6 ± 1.9 (96 ± 19%)	29.7 ± 3.8 (99 ± 12%)	45.7 ± 2.6 (91 ± 5%)	65.1 ± 3.5 (93 ± 5%)	81.4 ± 2.8 (90 ± 3%)
BTC-mPEG 5 kDa	10.8 ± 1.3 (108 ± 13%)	29.1 ± 5.6 (97 ± 19%)	50.6 ± 5.2 (101 ± 10%)	63.7 ± 3.1 (91 ± 4%)	85.6 ± 6.7 (95 ± 7%)
SPA-mPEG 5 kDa	11.9 ± 2.6 (119 ± 26%)	30.1 ± 5.7 (100 ± 19%)	50.2 ± 7.8 (100 ± 16%)	70.0 ± 7.6 (100 ± 11%)	84.6 ± 6.1 (94 ± 7%)
BTC-mPEG 20 kDa	12.0 ± 2.4 (120 ± 24%)	31.2 ± 5.6 (104 ± 19%)	49.5 ± 8.2 (99 ± 16)	69.2 ± 5.6 (99 ± 8%)	84.3 ± 2.0 (94 ± 2%)
SPA-mPEG 20 kDa	9.7 ± 1.6 (97 ± 16%)	30.0 ± 6.1 (100 ± 20)	47.6 ± 7.3 (95 ± 14)	65.4 ± 3.9 (93 ± 6%)	84.7 ± 4.3 (94 ± 5%)

To determine the ability to separate mPEG-modified cells from unmodified control cells, cell mixing experiments were done. ^{51}Cr-Labeled PEGylated RBC (2.5 mM mPEG 5 kDa or 0.9 mM mPEG 20 kDa) were prepared and mixed at the indicated percentages with ^{51}Cr-labeled unmodified control RBC. Cell mixtures were subjected to two-phase partitioning. The values shown represent the actual percentage of RBC in the upper PEG-rich phase. Values in parentheses represent the percent theoretical maximum recovery of the PEGylated ^{51}Cr-RBC.

the necessity of removing unmodified or insufficiently modified RBC. As demonstrated in Table 1, the two-phase partitioning system is ideally suited for this task as mixtures of mPEG-modified RBC and unmodified RBC were successfully separated. Following two-phase separation, approx. 90% of mPEG-derivatized RBC were readily recovered from the PEG-rich layer by removing the top phase, diluting this phase in saline, then concentrating the RBC by low speed centrifugation.

Particle electrophoresis data (Fig. 4) for mPEG-RBC with varying mPEG chain sizes demonstrated that mobility shifts were directly related to the polymer molecular mass. While larger polymers yielded larger shifts in RBC mobility towards zero, smaller polymers yielded small mobility decrements (regardless of the linker used). For example, the loss of approx. 50% of the inherent RBC mobility (i.e. from −1.2 to −0.6 μm·cm/V·s) was achieved by addition of as little as 0.3 mM BTC-mPEG 20 kDa as compared with ∼2 mM BTC-mPEG 5 kDa (Fig. 4A). Similarly, only 0.3 mM SPA-mPEG 20 kDa is required versus 2.5 mM SPA-mPEG 5 kDa. Derivatization of RBC with the short SPA-mPEG 2 kDa derivative was insufficient at the highest concentration tested to lower the mobility to 0.6 μm·cm/V·s (Fig. 4B). Indeed, substantially higher numbers of total ethoxy units were required for the PEG 5 kDa derivatives ((2.1:1), SPA-PEG 5 kDa:SPA-PEG 20 kDa).

In addition to the monofunctional derivatives employed, bifunctional PEG derivatives were also investigated. Fig. 5 demonstrates that RBC surface modification is readily achieved using the bifunctional BTC-PEG 3.4 kDa-BTC and SPA-PEG 3.4 kDa-SPA compounds. Electrophoretic mobility shifts for RBC modified with these bifunctional derivatives were, as might be expected, between those for the monofunctional 5 kDa and 2 kDa SPA-mPEGs (Figs. 5A and 4A). Whether RBC were modified with BTC- or SPA-PEG bifunctional derivatives, mobility profiles were comparable. Similarly, two-phase partitioning patterns for the bifunctional PEG 3.4 kDa-derivatized RBC were indistinguishable from one another (Fig. 5B). Unexpectedly, however, the bifunctional derivatives actually enhanced antiserum-mediated aggregation (Fig. 5C). Due to the presence of the two linker groups, a high degree

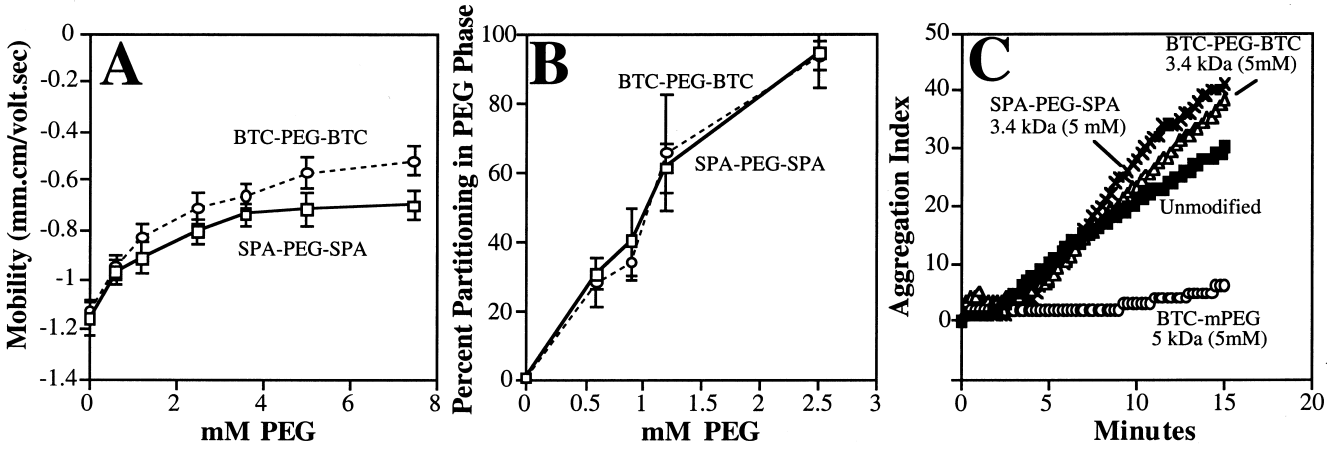

Fig. 5. Modification of RBC with bifunctional PEG derivatives adversely affects the RBC. RBC (washed and at a 12% hematocrit) were modified with the bifunctional BTC-PEG-BTC or SPA-PEG-SPA derivatives. In both cases the polymer size was 3.4 kDa. (A) As expected by the polymer size, the shift in electrophoretic mobility of the bifunctional mPEG derivatives was intermediate between the 2 and 5 kDa SPA-mPEG. However, it was observed microscopically during these studies that a significant percentage of the cells were aggregated together do to PEG cross-linking. (B) Grafting of the bifunctional PEG polymers to the RBC membrane resulted in the expected partitioning of the modified RBC to the PEG-rich phase. (C) The effect of RBC cross-linking and microaggregate formation due to the bifunctional derivatives was apparent in RBC aggregation studies. As shown, both the SPA-PEG-SPA and BTC-PEG-BTC bifunctional derivatives (5 mM derivatization concentration) actually enhanced type A RBC aggregation in response to anti-A serum. In contrast, the monofunctional BTC-mPEG (5 mM) completely inhibited antiserum-mediated agglutination under the same conditions. Consequent to these studies, the use of these bifunctional derivatives was discontinued. Symbols for panels A and B show the mean data for three experiments ±1 S.D., each done in duplicate. Microaggregation data are representative of three independent assays. Derivatized RBC shown were modified with 5.0 mM of the PEG derivative indicated.

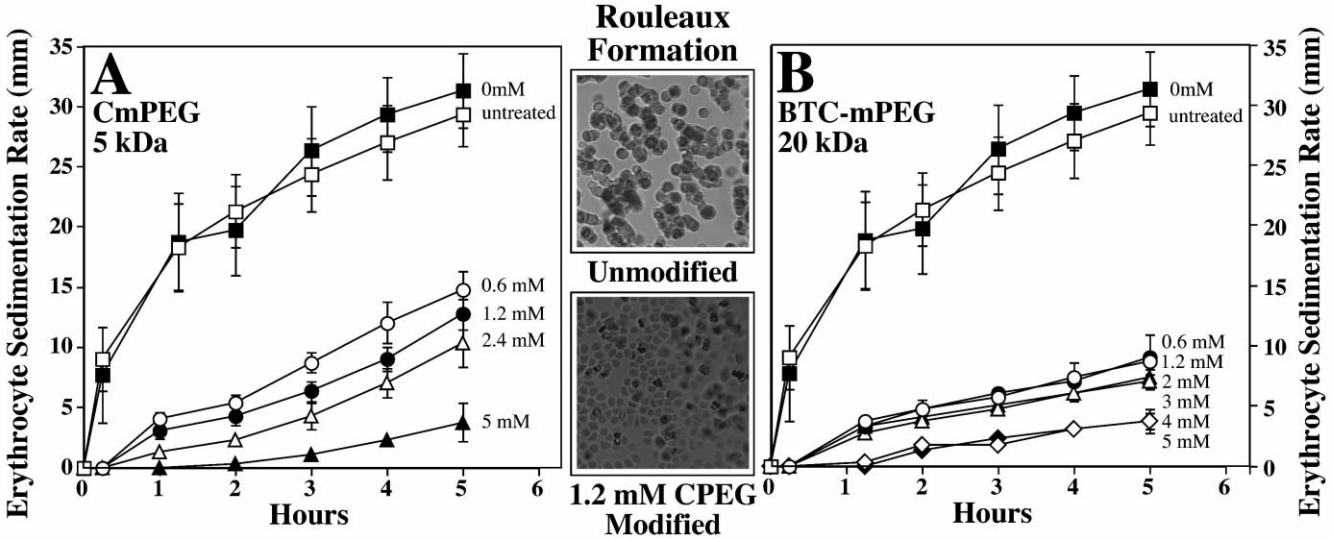

Fig. 6. Increasing polymer size prevents RBC sedimentation and Rouleaux formation. In vitro (in the presence of dextran) and in vivo, RBC self-associate giving rise to RBC 'stacks' (Rouleaux formation). In turn, the Rouleaux formation underlies RBC sedimentation. For analysis of sedimentation rate, control and mPEG-RBC (RBC modified as washed cells at a 12% hematocrit) were suspended to a 40% hematocrit in autologous plasma and loaded into erythrocyte sedimentation tubes. RBC sedimentation rate was then monitored over a 5 h period. Simultaneously, aliquots of the control and mPEG-derivatized RBC were mixed with equal amounts of either autologous plasma or a 1% saline-buffered dextran solution (to induce Rouleaux formation) and examined microscopically for Rouleaux formation.

of RBC-RBC cross-linkage was noted. Indeed, microscopic analysis conducted during the particle electrophoresis studies demonstrated numerous small aggregates of RBC.

The effect of linker chemistry and polymer size on Rouleaux formation and sedimentation rate was also assessed. Microscopic examination of the modified RBC demonstrated that cell–cell interactions were disrupted consequent to mPEG derivatization. This is graphically observed via Rouleaux formation in which RBC self-aggregate to form stacks of cells. As shown in Fig. 6, normal, unmodified RBC readily form Rouleaux structures in the presence of dextran. In contrast, mPEG modification inhibits the cell–cell interactions required for Rouleaux formation leading to the random distribution of cells in the microscope field. Consequent to the loss of Rouleaux formation, erythrocyte sedimentation rate (ESR) is significantly diminished in a dose-dependent manner. As shown in Fig. 6A, C-mPEG 5 kDa significantly decreases the ESR as a function of mPEG dose. The loss/delay in sedimentation rate is significant ($P < 0.01$) even at 0.6 mM of derivatization. However, even at this low derivatization dosage, self-association and sedimentation do occur with

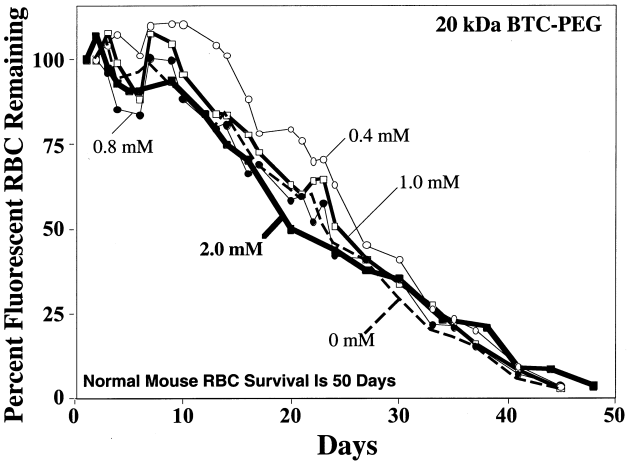

Fig. 7. In vivo survival of mouse mPEG-modified RBC is normal at immunoprotective levels of derivatization (2 mM) with BTC-mPEG 20 kDa. In vivo survival of mPEG-derivatized mouse RBC is normal even after repeated infusions. Shown are the clearance rates of transfused control and BTC-mPEG 20 kDa-modified mouse RBC. Survival was followed using a fluorescent fatty acid label (PKH-26) as described in Section 2. Each infusion approximated 8–10% of the total mouse RBC mass (based on weight and calculated blood volume). Following each RBC administration, cell clearance was allowed to proceed until no detectable label remained (approx. 50 days). Each time point represents the mean of a minimum of five Balb/c mice. Murine RBC survival studies utilized both i.v. and i.p. transfusion of the donor cells with no differences in survival kinetics noted between the two modes of administration.

time as noted by the difference between 1 and 5 h of sedimentation in the 0.6 mM-modified RBC. In contrast, subsequent to derivatization with BTC-mPEG 20 kDa, only a minor increase in sedimentation occurs over 5 h of incubation (Fig. 6B). These latter results clearly demonstrate the efficient disruption of cell–cell (Rouleaux) association by the larger polymers.

Surprisingly, in vivo survival studies also demonstrated that BTC-mPEG 20 kDa was vastly superior to the lower molecular mass (5 kDa) C-mPEG derivatives using the exact same modification conditions. As previously reported by us [5], C-mPEG 5 kDa derivatization of murine RBC at concentrations ≥0.6 mM gave rise to significantly shortened in vivo survival. In part, the loss of viability resulted from the inherently fragile nature of murine RBC. However, modification of the linker chemistry as well as the use of longer polymers results in significantly improved in vivo survival of murine RBC. As

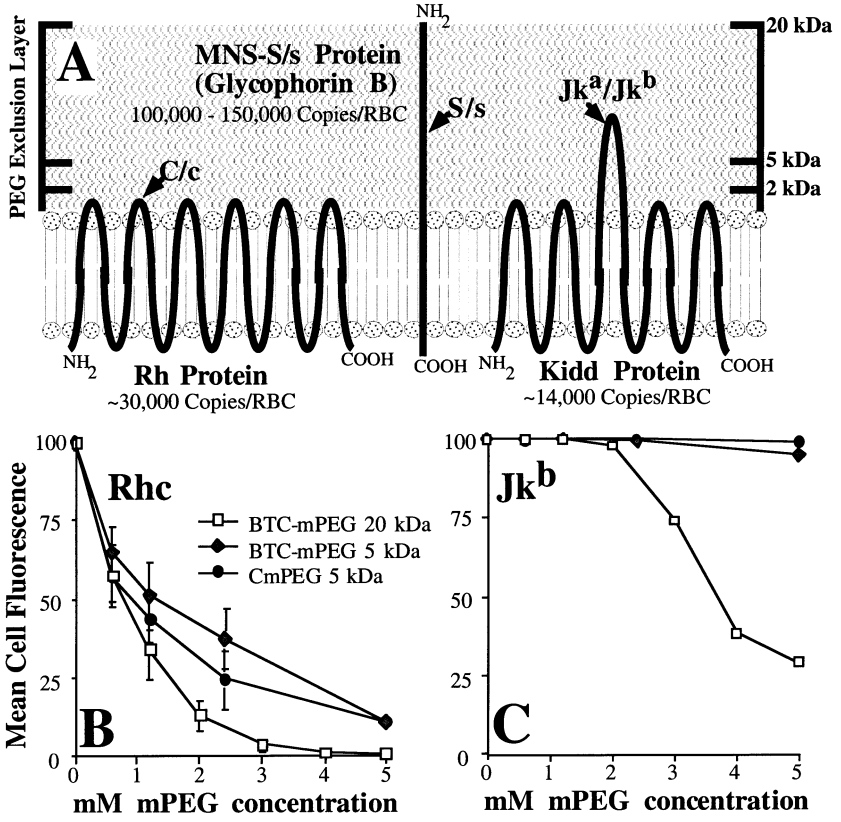

Fig. 8. Immunocamouflage of membrane antigens is a function of linker chemistry, polymer size, and polymer surface density. (A) Shown is a graphical representation of the RBC membrane and the topical distribution of the Rh (C/c), Kidd ($Jk^{a/b}$) and MNS (S/s) blood group antigens. The PEG exclusion layer is the physical entity which gives rise to the immunocamouflage of the membrane antigens. The efficacy of the heavily hydrated, neutrally charged, exclusion layer is a function of the length and density of the highly mobile PEG polymer which imparts a space filling (i.e. steric hindrance) cloud around the cell. Indeed, the PEG exclusion layer acts as a molecular size sieve allowing small molecules (e.g. O_2 and glucose) and proteins to efficiently cross while excluding larger proteins (e.g. antibodies). Similarly, the obfuscation of the inherent surface charge (Fig. 4) of the cell membrane by the neutral PEG layer is also of importance in preventing both antibody–antigen interaction and cell–cell interaction. Represented are the relative exclusion layers of 2, 5 and 20 kDa polymers. (B) The Rh antigens are located close to the membrane surface, consequently even relatively short polymers (e.g. 5 kDa) can effectively camouflage these sites. Shown is the immunocamouflage of the Rhc antigen as reflected by the decrease in mean cell fluorescence. As noted, both 5 kDa polymers similarly camouflaged the Rhc antigen. While increased polymer length (20 kDa) improved the immunocamouflage of the Rh antigens, the effect was moderate. (C) In contrast to the Rh antigens, polymer length was a critical determinant in the immunocamouflage of the MNS and Kidd blood group antigens. As demonstrated, neither 5 kDa polymer resulted in the immunocamouflage of the Jk^b antigen. In contrast, the 20 kDa polymer began to exert an efficient immunocamouflage of Jk^b.

shown in Fig. 7, in vivo survival studies using the 20 kDa BTC-mPEG resulted in normal survival kinetics (i.e. ~50 days) even at a derivatization concentration of 2 mM. Importantly, these in vivo data demonstrate that normal survival of cells is readily achievable at derivatization concentrations that impart an effective immunocamouflage of human RBC. Furthermore, as demonstrated by our previous studies, PEGylation of murine RBC also does not generate any neoantigens [4,20].

Finally, we investigated the effects of membrane topography on the efficacy of mPEG-mediated immunocamouflage. Inhibition of antibody binding to Rhc and JK^b consequent to mPEG derivatization was assessed via flow cytometry. While Rhc resides close to the lipid bilayer, JK^b is present well above the membrane (Fig. 8). For Rhc, inhibition of antibody binding was mPEG dose-dependent with increasing chain length (molecular mass) having only a small enhancing effect (Fig. 8B). In contrast, for antigenic determinants farther out from the lipid bilayer, the 5 kDa mPEGs were completely ineffective, regardless of chain density. However, as demonstrated with the 20 kDa BTC-mPEG, with increasing chain length and density, increasing immunocamouflage was observed (Fig. 8C). These findings clearly illustrate the importance of antigen topography on the efficacy of immunocamouflage and perhaps indicate why the murine cells derivatized with 20 kDa BTC-mPEG have improved survival when compared to the 5 kDa derivatized cells.

4. Discussion

Characterizing, quantifying and controlling the biophysical and immunological consequences of mPEG derivatization of RBC are vital for the successful application of this novel technology in transfusion medicine. To this end, the biophysical and biological efficacy of three different chemical linkers with different polymer lengths (molecular mass) was assessed via particle electrophoresis, aqueous two-phase partitioning, sedimentation rate and in vivo survival.

The chemical linkers used to activate the mPEG (C-, BTC-, and SPA-mPEG) for covalent binding of the polymer to proteins all preferentially target the ε-amino group of exposed lysine residues on membrane proteins. While sharing the same targets, BTC- and SPA-mPEGs differ from C-mPEG in that they attach mPEG directly to the lysine residue without introducing a bulky linker moiety. Comparison of the mPEG 5 kDa derivatives demonstrated that C-mPEG reacted most rapidly but, given appropriate derivatization time (1 h versus 30 min), SPA- and BTC-mPEG-modified RBC exhibited similar biophysical (particle electrophoresis, phase partitioning) and immunological (inhibition of Rouleaux formation and non-ABO antigen detection) characteristics (Figs. 2–4, 6 and 8). Hence, any of these monofunctional linkers could be suitable for RBC derivatization in the clinical setting.

Other important findings relate to the effects of polymer size; i.e. size does matter. Larger polymers were found to more effectively camouflage RBC as demonstrated by both biophysical and immunological measurements. While both particle electrophoresis and partitioning results demonstrated that smaller quantities of the larger PEG derivatives were required to exert significant PEG-specific effects, particle electrophoresis proved to be more sensitive to PEG derivative molecular mass changes than partitioning. For example, a 4-fold increase in mPEG derivative molecular mass (from 5 kDa to 20 kDa) resulted in the requirement of 7–8 times less mPEG derivative to achieve a 50% shift in cell mobility. In contrast, the same 4-fold increase in the polymer size resulted in only a 3–4-fold decrease in the derivative concentration required to achieve 80% partitioning into the PEG-rich phase.

This heightened effect of mPEG molecular mass demonstrated by particle electrophoresis may also be discussed as a function of the number of ethoxy units. Less than half of the total ethoxy units were required for mPEG 20 kDa derivatives compared to mPEG 5 kDa derivatives to decrease the cell mobility by 50%. The greater inhibition of cell mobility by the large PEGs is likely due to the much greater drag force contributed by the longer polymers. In contrast, in the affinity partitioning system, slightly more of the larger PEGs were required (beyond that required to give an equivalent number of ethoxy units). Since the affinity partitioning of mPEG-RBC into the PEG-rich phase is related to the number of ethoxy units attached, these data may reflect that

fewer of the 20 kDa derivative molecules are attached. This finding was expected as the binding of a few mPEG 20 kDa polymers is likely to sterically inhibit the approach and binding of further molecules over a much larger surface area of the cell. In contrast, the smaller molecular mass mPEG derivatives sterically inhibit over a much smaller membrane surface area thus allowing for the approach and binding of more polymers.

In contrast to the monofunctional mPEG derivatives, bifunctional PEGs were not suitable for RBC-PEGylation using current conditions. At the ratios used for modifying RBC, the two bifunctional derivatives, BTC-mPEG 3.4 kDa-BTC and SPA-mPEG 3.4 kDa-SPA, were found to cross-link RBC during the derivatization procedure. This cross-linking effectively interfered with the ability of PEG to keep cells apart from one another (which is the key to inhibiting agglutination since the anti-A antibody still binds the type A PEG-modified RBC [10]). Consequently, when anti-A antibodies are added in the agglutination reaction, inhibition of the antibody-mediated cell–cell interaction is not seen. Agglutination would also be amplified due to the pre-existence of small RBC aggregates. We hypothesize that, in some circumstances, these bifunctional PEG derivatives may prove useful if RBC numbers are significantly reduced (i.e. diluted) to minimize cell–cell cross-linking.

As predicted by these studies, the immunocamouflage of RBC membrane antigens is determined by the number of grafted mPEG molecules, polymer size (i.e. molecular mass), antigen density and antigen topography (i.e. the relative height of the antigen above the membrane surface). These findings are graphically presented in Fig. 8. As demonstrated in this figure, antigenic and immunogenic epitopes such as human RhC/c (as well as other Rh antigens; Fig. 8A,B) which are close to the membrane surface are effectively camouflaged by both short and long chain polymers at low to medium levels of derivatization. Hence, antigens such as RhC that statistically exhibit an approx. 5% risk of alloimmunization after a single transfusion, should show a dramatically decreased risk following RBC PEGylation. In contrast, other antigens such as the Kidd and MNS blood group antigens that extend well above the membrane are less efficiently camouflaged by the short chain polymers but can be effectively hidden by the longer chain polymers (Fig. 8A,C). To what extent RBC PEGylation will attenuate alloimmunization to these later antigens remains unclear. However, antigenic recognition and immunogenicity are not the same. Importantly with regard to this question, we have previously demonstrated that antibody formation (i.e. immunogenicity) in response to PEGylated allogeneic and xenogeneic RBC in mice is effectively blunted [19], suggesting that even epitopes far away from the membrane are protected from immunologic presentation consequent to membrane derivatization.

Of equal importance to the potential clinical applications of mPEG-RBC is the effect of PEGylation on cell–cell interactions. As described herein, Rouleaux formation as well as antibody-mediated RBC–RBC interactions were effectively blocked by mPEG modification. These findings may have implications with regard to the vasoocclusive events characteristic of sickle cell disease. In sickle cell disease, vasoocclusive events are mediated by the enhanced viscosity and aggregation of abnormal RBC in the small arterioles and capillaries. However, as we have recently demonstrated, PEG-RBC serve as efficient chain breakers during aggregation of unmodified RBC [19]. Hence, consequent to the PEG exclusion volume, RBC retain better flow characteristics in the arterioles, resist agglutination, and do not adhere to endothelial surfaces. Indeed, an excellent study by Armstrong et al. [21] clearly demonstrated that mPEG modification reduces low shear viscosity. This loss of viscosity is clearly due to impaired cell–cell interaction as readily evidenced by the loss of Rouleaux formation and decreased sedimentation rate. Finally, the inhibition of cell–cell interactions (e.g. monocyte–RBC or antigen presenting cell–T lymphocyte) likely underlies the blunted immune response to mPEG-modified cells since immunorecognition requires both cell–cell and cell–antibody interactions for the induction of an efficient immunological response [4,6].

Finally, a critically important step in the potential clinical utilization of the PEG-RBC is the separation of modified (i.e. non-immunogenic) from unmodified/undermodified (i.e. immunogenic) cells. As demonstrated in this study, the biophysical changes arising from membrane derivatization allow for the rapid and efficient processing and recovery of immunocamouflaged (PEG-modified) RBC. For example,

mixtures of strongly PEGylated cells (2.5 mM PEG 5 kDa or 0.9 mM PEG 20 kDa derivatives) and unmodified cells were easily and efficiently separated by aqueous two-phase partitioning. mPEG-RBC in the upper, PEG-rich phase were then recovered by diluting the PEG phase in saline (to decrease the viscosity) followed by low speed centrifugation. Importantly, this simple method for separating and recovering PEG-modified RBC can be readily scaled up to manufacturing proportions as was previously done for enzymes (e.g. phosphorylase, several dehydrogenases) purified from microorganisms [22].

In sum, multiple linker molecules (cyanuric chloride, BTC, and SPA) were all efficient at derivatizing RBC membranes with mPEG. No significant differences, other than rate of reaction, were observed between the linker moieties when comparable polymer sizes were assessed via particle electrophoresis, two-phase partitioning, and immunological analyses. Both polymer surface density and polymer size significantly influenced the biophysical (electrophoretic mobility, phase partitioning, and cell–cell interaction) and immunological characteristics of modified RBC. While it was anticipated that larger polymers would achieve better immunocamouflage, we were pleasantly surprised that the larger polymers also exhibited improved in vivo viability at equimolar concentration. Furthermore, these data suggest that the derivatization and purification of mPEG-RBC can be efficiently and economically done in the Blood Bank setting. Clinical usage of these modified cells may have tremendous therapeutic advantage in managing sickle cell disease which is aggravated by significant disparities in non-ABO antigens and vaso-occlusive events arising from enhanced cell–cell interactions.

Acknowledgements

The authors thank Raymond Norris-Jones and Dr. Donald E. Brooks of the University of British Columbia for advice on two-phase partitioning and for access to particle electrophoresis equipment. This work was supported by National Institutes of Health Grant HL58584 (M.D.S.) and the Cooley's Anemia Foundation (K.L.M.).

References

[1] H. Teppler, G. Kaplan, K.A. Smith, A.L. Montana, P. Meyn, Z.A. Cohn, J. Exp. Med. 177 (1993) 483–492.
[2] F.H. Brucato, S.V. Pizzo, Blood 76 (1990) 73–79.
[3] A. Gabizon, D. Papahadjopoulos, Proc. Natl. Acad. Sci. USA 85 (1988) 6949–6953.
[4] M.D. Scott, K.L. Murad, F. Koumporouras, M. Talbot, J.W. Eaton, Proc. Natl. Acad. Sci. USA 94 (1997) 7566–7571.
[5] K.L. Murad, K.L. Mahany, C. Brugnara, F.A. Kuypers, J.W. Eaton, M.D. Scott, Blood 93 (1999) 2121–2127.
[6] K.L. Murad, E.J. Gosselin, J.W. Eaton, M.D. Scott, Blood 94 (1999) 2135–2141.
[7] E.P. Vichinsky, A. Earles, R.A. Johnson, M.S. Hoag, A. Williams, B. Lubin, New Engl. J. Med. 322 (1990) 1617–1621.
[8] G. Sirchia, A. Zanella, A. Parravicini, F. Morelati, P. Rebulla, G. Masera, Transfusion 25 (1985) 110–112.
[9] K. Maruyama, T. Yuda, A. Okamoto, C. Ishikura, S. Kojima, M. Iwatsuru, Chem. Pharm. Bull. 39 (1991) 1620–1622.
[10] A.J. Bradley, S.T. Test, K.L. Murad, J. Mitsuyoshi, M.D. Scott, Transfusion 41 (2001) 1225–1233.
[11] C. Delgado, F. Malikk, B. Selisko, D. Fisher, G.E. Francis, J. Biochem. Methods 29 (1994) 237–250.
[12] K. Moribe, K. Maruyama, M. Iwatsuru, Chem. Pharm. Bull. 45 (1997) 1683–1687.
[13] J. Janzen, X. Song, D.E. Brooks, Biophys. J. 70 (1996) 313–320.
[14] H. Walter, E.J. Krob, Biochim. Biophys. Acta 455 (1976) 8–23.
[15] E. Eriksson, P.A. Albertsson, G. Johansson, Mol. Cell. Biochem. 10 (1976) 123–128.
[16] D.E. Brooks, R. Norris-Jones, Methods Enzymol. 228 (1994) 14–27.
[17] P. Lutwtche, R. Norris-Jones, D.E. Brooks, Appl. Environ. Micro. 61 (1995) 3251–3255.
[18] G.V.F. Seaman, in: D.M. Surgenor (Ed.), The Red Blood Cell, Academic Press, New York, 1975, pp. 1135–1161.
[19] M.D. Scott, A.J. Bradley, K.L. Murad, Transfus. Med. Rev. 14 (2000) 53–63.
[20] M.D. Scott, K.L. Murad, Curr. Pharm. Des. 4 (1998) 423–438.
[21] J.K. Armstrong, H.J. Meiselman, T.C. Fisher, Am. J. Hematol. 56 (1997) 26–36.
[22] H. Hustedt, K.H. Kroner, M.-R. Kula, in: H. Walter, D.E. Brooks, D. Fisher (Eds.), Partitioning in Aqueous Two-phase Systems. Theory, Methods, Uses, and Applications to Biotechnology, Academic Press, New York, 1985, pp. 529–584.